2021 43rd Annual International Conference of the
IEEE Engineering in Medicine & Biology Society (EMBC)
Oct 31 - Nov 4, 2021. Virtual Conference

The Effect of Electrical Stimulation on the Response of Mouse Retinal Ganglion Cells

Wanying Li[#], Zhen Xu[#], Hao Wang*, Tianzhun Wu*, *Senior Member, IEEE*

***Abstract*— Retinal prostheses can restore the basic visual function of patients with retinal degeneration, which relies on effective electrical stimulation to evoke the physiological activities of retinal ganglion cells (RGCs). Current electrical stimulation strategies suffer from unstable effects and insufficient stimulation positions. Therefore, it is crucial to determine the optimal parameters for precise and safe electrical stimulation. Biphasic voltages (cathode-first) with a pulse width of 25 ms and different amplitudes were used to *ex vivo* stimulate RGCs of three wild-type (WT) mice using a commercial microelectrode array (MEA) recording system. Based on a facile and efficient spike sorting method, comprehensive statistics of RGCs response types were performed, and the influence of electrical stimulation on RGCs response status was analyzed. There were three types of RGCs response measured from the retinas of three WT mice, and the proportions were calculated to be 91.5%, 3.11% and 5.39%, respectively. This work can provide an in-depth understanding of the internal effects of electrical stimulation and RGCs response, with the potential as a useful guidance for optimizing parameters of electrical stimulation strategies in retinal prostheses.**

I. INTRODUCTION

Retinitis pigmentosa (RP) and age-related macular degeneration (AMD) are retinal degeneration (RD) diseases with a prevalence of more than 1/4000 [1-3]. The photoreceptor cells of RP and AMD patients degenerate irreversibly and cannot convert optical inputs into neural spikes, resulting in the loss of part or even all visual functions. However, even for profound RD patients, some physiological structures and functions of the retinal ganglion cells (RGC) are usually still preserved [4]. Therefore, the RGC can be stimulated to evoke the neural activity of the remaining retinal neurons [5, 6], thereby providing a straightforward method for the blind to restore visual function.

Such retinal stimulation methods that have been used to restore visual functions include electrical stimulation [4, 7, 8], optogenetics, photochemistry, ultrasonic stimulation, etc. Particularly, electrical stimulation based retinal prosthesis have been well studied for decades and recognized as the mainstream for practical applications. In recent years, such retinal prostheses have achieved great progress in the device safety, integration and miniaturization. In addition, many clinical trials and commercial implantation about the retinal prostheses have been reported [9, 10].

For electrical stimulation of retinal prostheses, current stimulation strategies (waveform, amplitude, etc.) have some shortcomings such as unstable effects and inaccurate stimulation positions [12]. Therefore, it is crucial to determine the appropriate stimulation parameters for better performances. Many researches on optimizing electrical stimulation parameters have been reported [3, 13]. For example, Archana *et al.* explored the effects of stimulation parameters (voltage amplitude, duration and polarity) on mice RGCs, and concluded that the optimal parameters were the one corresponding to the maximum number of activated RGCs. However, they only performed relevant statistics and analysis on the activated response of RGCs, without considering other responses. For the optimization of electrical stimulation strategies, it is vital to understand the influence of parameters on the various types of response RGCs.

In addition, some studies have shown that electrical stimulation strategies can also be optimized by exploring the relationship between stimulation parameters and RGC early response (defined as spikes are evoked by RGC within 100 ms in post-stimulation) [14, 15]. For example, Yong *et al.* studied the effects of voltage stimulation and current stimulation (with variable: amplitudes and durations) on the early response of mice RGCs, respectively, to determine the optimal stimulation parameters. However, they focused only on the RGCs early responses evoked by electrical stimulation, lacking the analysis of late responses (*i.e.*, the spikes evoked after 100 ms in the post-stimulation). However, it has been found that the late response also affected the performance of electrical stimulation [16]. Therefore, the optimization of parameters needs to be achieved by exploring the influence of electrical stimulation on the late response of RGCs.

Considering the limitations of current research, this work mainly focuses on two goals: (1) Comprehensive statistics on the types of RGCs responses, and analysis the impact of electrical stimulation on RGC response status. (2) Perform spike detection, spike classification and visualization for late response of RGC signal. In general, we anticipate that this study can provide effective guidance for determining the optimal parameters for retinal electrical stimulation.

* Corresponding author.
# These authors contributed equally to this work.
Wanying Li and Zhen Xu are with Institute of Biomedical and Health Engineering, Shenzhen Institute of Advanced Technology, Chinese Academy of Sciences, Shenzhen, China (e-mail: wy.li2@siat.ac.cn, zhen.xu@siat.ac.cn).
Hao Wang* and Tianzhun Wu* are with Institute of Biomedical and Health Engineering, Shenzhen Institute of Advanced Technology, Chinese Academy of Sciences, Shenzhen, China (phone: +86-755-86585211; hao.wang@siat.ac.cn. phone: +86-755-86392339; fax: +86-755-8639-2339; e-mail: tz.wu@siat.ac.cn.).

II. EXPERIMENT SETUP AND DATA COLLECTION

A. Sample preparation

In this study, three 12-week-old C57BL/6J wild-type (WT) mice were used for the ex vivo experiment. The mice were anesthetized by the injection of a mixture of ketamine (50 mg/kg) and xylazine (10 mg/kg), then the eyeballs were removed, and the retina was finally cut into four parts and attached to a filter membrane against the photoreceptor layer. The ganglion cell layer in the retina was inverted and placed on a commercial MEA. The animal experiments in this study had been approved by Institutional Animal Care and Use Committee of Shenzhen Institution of Advanced Technology, Chinese Academy of Sciences (Approval number SIAT-IRB-180301-YGS-XUZHEN-A0244).

B. Electrical stimulation and recording

The MEA is connected to the MEA2100 data processing system, and the MC-Rack software is used for electrical stimulation of a single electrode and signal recording of 120 electrodes (Fig. 1). The sampling frequency of electrical stimulation signals is 10 kHz/channel. The voltage used is a two-phase pulse (cathode first), and the voltage amplitudes of the cathode and anode pulses are set to A and $A/2$, respectively. In detail, the range of A is 0.15 V to 1.65 V with 0.15 V steps, and lasts 25 ms [17]. On the other hand, the anode pulse duration is 50ms, and all injected charges will be neutralized. During the experiment, all voltages will be repeated 20 times, and the interval between two consecutive stimulations is 10s. The MEA recorded a total of 1s of RGCs signals, *i.e.*, spontaneous of 0.1s in pre-stimulation and 0.9s in post-stimulation. In this work, a total of 17 central electrode signals were stimulated.

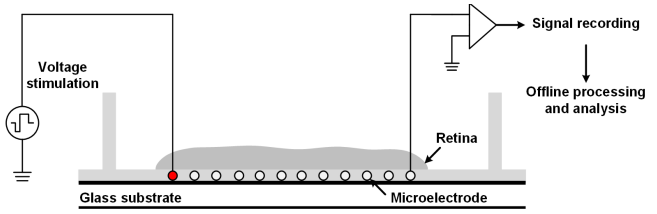

Fig. 1. Experimental setup and illustration. One electrode performs electrical stimulation on the retinal ganglion layer (marked in red), and all other electrodes can record neural signals from the ganglion cells.

III. METHOD

A. Signal preprocessing

The main purpose of preprocessing is to remove artifacts caused by electrical stimulation. Generally speaking, since electrical stimulation produces disturbances to the stimulation location and surroundings, there are signal traces much larger than spikes near the stimulation location. In this paper, these artifacts are retrieved and reset to zero. The signal obtained by preprocessing will be used for subsequent spike detection and clustering operations.

B. Spike detection

The previously reported method [18] was used to detect the spikes of the preprocessed signal to obtain the spikes waveforms evoked by RGC. This method is mainly composed of stationary wavelet transform and Teager energy operator. For stationary wavelet transform, there is translation invariance, which can effectively reduce the adverse effects caused by noise. In addition, the Teager energy operator is often used to estimate the transient energy of the signal, which can better separate the spike signal from the background noise. In summary, the method proved to be facile and effective, and was used to complete spike detection.

C. Feature extraction

In order to better realize the visualization of a single RGC unit, this paper updates the feature extraction and clustering procedures based on [18]. Due to the huge number of signals obtained by spike detection, containing redundant information and high correlation, it directly leads to misclassification. Therefore, the features extracted from the signal need to be used as the input to improve the performance of clustering. Generally, without losing the original main information, data reduction can be achieved by principal component analysis (PCA), which can be used as the method of feature extraction in this work [19].

Through the eigenvalue decomposition of the covariance matrix, PCA can linearly convert the input signal into an uncorrelated variable (principal component, PC). PCs are the most informative data in the original signal, which can provide useful discrimination for clustering. The extracting features (PCs) are shown in Fig. 2 (a) [20]:

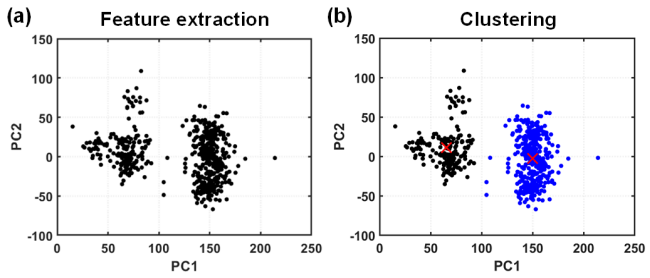

Fig 2. The extracted features are separated into single-unit. (a) The PCs in two-dimension of the extracted features are displayed. (b) The clustering result of the GMM method.

D. Clustering

The purpose of clustering is to divide the extracted features into single units and assign each feature to the corresponding class, which can analyze the activity of a single-unit. Based on the parameter probability density function, *i.e.*, the weighted sum of Gaussian component density, the Gaussian mixture model (GMM) performs clustering by approximately calculating the probability distribution of the extracted features [21]. The process of GMM is illustrated as follow [22], and the clustering result of extracting features is shown in Fig. 2 (b).

The *n*-dimensional dataset is composed of the extracted features *X*. For each Gaussian component *i*, the probability density function is calculated by Eq. 3, where μ_i and $\sum_i$ represent the mathematical expectation and covariance matrix, respectively.

$$g(X|\mu_i,\sum_i)=\frac{1}{(2\pi)^{\frac{n}{2}}\left|\sum_i\right|^{\frac{1}{2}}}exp(-\frac{1}{2}(X-\mu_i)^T\sum_i^{-1}(X-\mu_i)) \quad (3)$$

Meanwhile, the probability density function of GMM with *K* components is given by Eq. 4, where $\lambda=\{\omega_i,\mu_i,\sum_i\}$ represents the mixing parameters of GMM, estimated by maximizing the log-likelihood function (Eq. 5). In addition, ω_i (i = 1, …, K) is mixing weight of *K* components, meeting this constraint: $\sum_{i=1}^{K}\omega_i=1$.

$$p(X\mid\lambda)=\sum_{i=1}^{K}\omega_i g\left(X\mid\mu_i,\sum_i\right) \quad (4)$$

$$L(X\mid\lambda)=ln[\sum_{i=1}^{K}\omega_i g(X\mid\mu_{i,}\sum_i)] \quad (5)$$

The expectation maximization (EM) algorithm is applied to solve the maximum likelihood estimation. The iterative process of EM is as follows:

1) Initialize the mixing parameters λ of GMM.

2) Expectation step: For each sample, the posterior probability of each Gaussian component *i* is determined by Eq. 6.

$$\Pr(i\mid X,\lambda)=\frac{\omega_i g(X\mid\mu_i,\sum_i)}{\sum_{j=1}^{K}\omega_j g(X\mid\mu_j,\sum_j)} \quad (6)$$

3) Maximization step: For each Gaussian component, the mixing parameters λ are updated by Eqs (7-9), where *N* Represents the number of samples in the dataset *X*.

$$\omega_i^{update}=\frac{1}{N}\sum_{j=1}^{N}\Pr(i\mid X_j,\lambda) \quad (7)$$

$$\mu_i^{update}=\frac{\sum_{j=1}^{N}\Pr(i\mid X_j,\lambda)X_j}{\sum_{j=1}^{N}\Pr(i\mid X_j,\lambda)} \quad (8)$$

$$\sum_i^{update}=\frac{\sum_{j=1}^{N}\Pr(i\mid X_j,\lambda)(X_j-\mu_i^{update})(X_j-\mu_i^{update})^T}{\sum_{j=1}^{N}\Pr(i\mid X_j,\lambda)} \quad (9)$$

4) Repeat step 2 and step 3 until the parameters λ convergence.

E. Raster plot and post-stimulus time histogram

After the clustering process the single-unit spike sequence was obtained. In this study, the raster plot (20 trials) is used to characterize the distribution of the spike evoked by the RGC unit, and generated from the spike firing time of the clustered RGC unit. In addition, the total number of spikes in different time periods in the raster plot is displayed by the post-stimulus time histogram (PSTH), which can also be used to quantify the firing rate of spikes (Fig. 3). Through the above visualization method, the response of RGC after electrical stimulation can be observed.

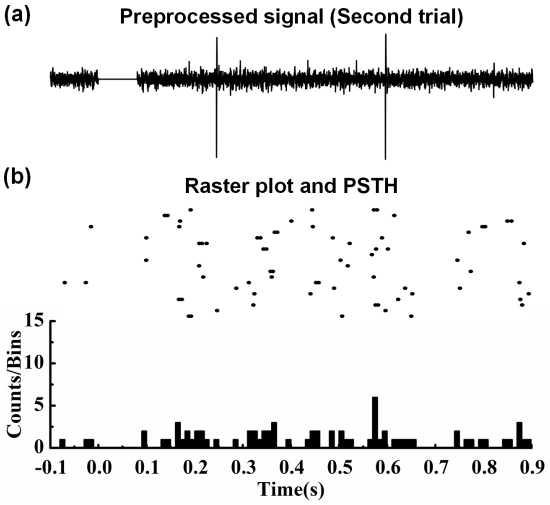

Fig 3. (a) Through spike detection, feature extraction and clustering, the spikes of RGC unit can be obtained from the preprocessed signal (Due to large artifact, the 0s-0.08s segment in the original signal is reset to zero). (b) The point in raster plot represents the spike was fired at the corresponding time in different trial, and the wide-bin window of PSTH is uniformly 10 ms. In addition, the electrical stimulation was performed at 0 seconds.

IV. RESULTS

Through the raster plot and PSTH, it can be known that there are mainly three types of response in the RGC unit after electrical stimulation. One of them is shown in Fig. 3 (b), which is considered as a spontaneous activity of the RGC unit. It can be seen that the spikes evoked by the RGC unit are scattering and irregular in 20 trials and are not concentrated in any timestamp. Moreover, the bin distribution in the PSTH is relatively uniform, and the number of corresponding spikes is equivalent. Therefore, the response of the RGC unit is called Type I when meeting the above conditions. In addition, the remaining two types are described in detail below.

A. The response types of RGC unit after electrical stimulation

Fig. 4 describes the second response type (called Type II) of the RGC unit. As shown in Fig. 4 (a), the spikes are concentrated between 0.1s and 0.2s (defined as the active zone), and the number of spikes in each trial is distributed in the range of 4 to 8. In addition, when the time exceeds 0.2s, the number of spikes decreases rapidly and disappears in multiple experiments. Furthermore, Fig. 4 (b) shows that each window in the active zone contains a different number of spikes. In other time interval, spikes are randomly evoked and the number is much less than the active zone. In summary, in the second response type, the spikes are excited at the activation zone, *i.e.*, close to the stimulation location, and does not exist in other time areas.

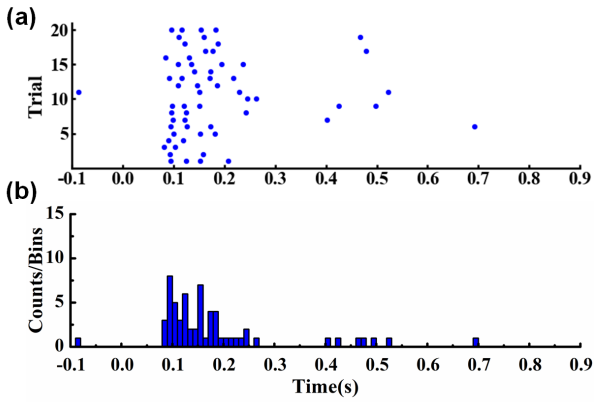

Fig 4. The second response type of (a) Raster plot and (b) PSTH.

A sample of the third response type (called Type III) in the RGC unit is shown in Fig. 5. Similar to the second type, the third response of the RGC unit also has an active zone. However, there will be a delay in the active zone, which usually occurs after 0.2s. Specifically, it can be seen from Fig. 5 (a) that the spike is evoked at a high firing rate between 0.3s and 0.4s, and the distribution in other time intervals is similar to the second type. In addition, Fig. 5 (b) shows that the number of each bin in the active zone exceeds 10. In short, this type of response generates an active zone far away from the stimulus timestamp, and the evoked spikes are random near the stimulus location (0.1s-0.2s).

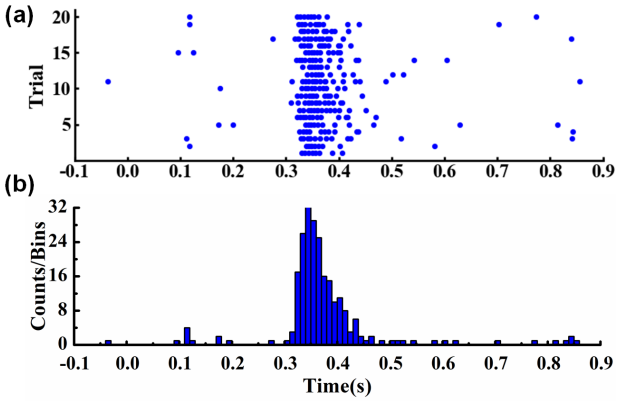

Fig 5. The third response type of (a) Raster plot and (b) PSTH.

B. Statistical results of different response type in RGC units

The statistical results of the three response types in RGC units are described in Table I. It can be seen that the total numbers of Type I for the three samples is 883, while the sums of Type II and Type III are 30 and 52, respectively. Particularly, the largest number of response types for RGC units in the three samples is Type I. In addition, for the total stimulus of sample 1 and sample 3, the number of Type III is greater than that of Type II, while the sum of the two types in sample 2 is similar. In summary, the response of the RGC unit after electrical stimulation is most probable for type I, possibly accompanied by the appearance of the remaining two types.

Table I. The number of each response type in RGC units.

WT mice	Stimulus	Type I	Type II	Type III
Sample 1	No.1	37	2	2
	No.2	28	2	5
	No.3	39	0	5
	No.4	19	5	11
	No.5	31	2	3
Sample 2	No.1	64	0	4
	No.2	72	2	0
	No.3	72	3	0
	No.4	65	4	6
	No.5	66	7	4
	No.6	73	0	4
Sample 3	No.1	65	0	0
	No.2	56	0	1
	No.3	47	1	0
	No.4	43	1	4
	No.5	53	0	1
	No.6	52	1	2
	Sum	882	30	52

V. DISCUSSION AND CONCLUSION

Regarding that the complete type of retinal RGCs response after electrical stimulation is not clear, it is of great significance to fully explore the impact of electrical stimulation on retinal RGCs. We performed electrical stimulation on the retinal ganglion cell layer of three WT mice (17 stimulation), and analyzed the type and number of late responses under each stimulation. This work has achieved the expected goals well, and the main contributions include: 1) Analyzes the RGC response through a facile and effective spike sorting method, and comprehensively statistics the response types, which has determined all response status of RGCs after electrical stimulation; 2) Performs the late response analysis of RGCs, which provided evidence for exploring the inner influence of electrical stimulation on the response of RGCs. The specific contributions of this paper will be discussed in detail as follows.

The signals recorded by MEA are used for spike detection, clustering and response analysis by the methods proposed in previous work [18]. The final result shows that there are three types of late response of RGC after electrical stimulation (Fig. 3-Fig. 5). First, Type I is the most common state of response, and it shows that electrical stimulation has almost no effect on RGC, accounting for approximately 91.5% of the three types (Table I). In addition, the numbers of Type II and Type III are similar, accounting for 3.11% and 5.39%, respectively. For the type II phenomenon, it can be explained that the electrical stimulation actively disturbs the RGC, which increases the frequency of spikes, and then the RGC returns to its initial status [23]. For Type III, we believe that the bipolar cells are stimulated, causing the spike to be evoked at a high firing rate after a short interval of silence [12]. For better-performing retinal prostheses, we hope that Type I will account for a large number, while Type II and Type III are as few as possible.

Many previous studies have explored the early response of RGC after electrical stimulation, but the work of Young *et al.*

shows that the late response is of great significance for evaluating the performance of retinal prostheses [16]. Therefore, this paper focuses on the analysis of the late response, which is useful for exploring the internal relationship between electrical stimulation and RGC response. In summary, the statistical analysis of all status in late response supplements the current research deficiencies, and provides new research ideas for evaluating the performance of retinal prostheses and improving stimulation strategies.

There are several research limitations. First, only the effect of electrical stimulation on the response type of WT mouse retina has been analyzed, yet that of retinal degeneration mice and the internal mechanism need to be fully explored. In addition, the relationship between response types and parameters needs further study by tuning appropriate electrical stimulation parameters (amplitude, duration, etc.) directly. Recently, five retinal degeneration mice have been used for the *ex vivo* experiments. In the near future, we will further explain the reasons for the emergence of multiple response types, and explore the correlation between different mice types and stimulation parameters, which provides effective solutions for improved stimulation strategies.

In conclusion, the study on the effect of electrical stimulation on the mouse retina can provide a comprehensive and in-depth understanding of the response mechanism in the retina. This work can provide a useful insight for achieving stable and precise electrical stimulation, and has the potential to determine an effective direction for improving the performance of retinal prostheses.

ACKNOWLEDGMENT

This study was financially supported by National Key Research and Development Program of China (2017YFC0111202), Shenzhen Science and Technology Research Program (JCYJ20170818152810899, JCYJ20170818154035069), Guangdong Science and Technology Research Program (2019A050503007), National Natural Science Foundation of China (31800871, 31900684), Grants of Chinese Academy of Sciences (172644KYSB20190077), and CAS Key Laboratory on Health Bioinformatics (2011DP173015).

REFERENCES

[1] D. T. Hartong, E. L. Berson, and T. P. Dryja, "Retinitis pigmentosa," *The Lancet,* vol. 368, no. 9549, pp. 1795-1809, 2006.

[2] D. Pascolini and S. P. Mariotti, "Global estimates of visual impairment: 2010," *Br. J. Ophthalmol.,* vol. 96, no. 5, pp. 614-618, 2012.

[3] A. Jalligampala, S. Sekhar, E. Zrenner, and D. L. Rathbun, "Optimal voltage stimulation parameters for network-mediated responses in wild type and rd10 mouse retinal ganglion cells," *Journal of neural engineering,* vol. 14, no. 2, p. 026004, 2017.

[4] K. Mathieson *et al.*, "Photovoltaic retinal prosthesis with high pixel density," *Nature photonics,* vol. 6, no. 6, pp. 391-397, 2012.

[5] S. T. Walston, R. H. Chow, and J. D. Weiland, "Direct measurement of bipolar cell responses to electrical stimulation in wholemount mouse retina," *Journal of neural engineering,* vol. 15, no. 4, p. 046003, 2018.

[6] C. M. Rountree, C. Meng, J. B. Troy, and L. Saggere, "Mechanical stimulation of the retina: therapeutic feasibility and cellular mechanism," *IEEE Transactions on Neural Systems and Rehabilitation Engineering,* vol. 26, no. 5, pp. 1075-1083, 2018.

[7] M. S. Humayun *et al.*, "Visual perception in a blind subject with a chronic microelectronic retinal prosthesis," *Vision research,* vol. 43, no. 24, pp. 2573-2581, 2003.

[8] Q. Zeng, S. Zhao, H. Yang, Y. Zhang, and T. Wu, "Micro/nano technologies for high-density retinal implant," *Micromachines,* vol. 10, no. 6, p. 419, 2019.

[9] E. Zrenner, "Will retinal implants restore vision?," *Science,* vol. 295, no. 5557, pp. 1022-1025, 2002.

[10] D. Boinagrov, S. Pangratz-Fuehrer, G. Goetz, and D. Palanker, "Selectivity of direct and network-mediated stimulation of the retinal ganglion cells with epi-, sub-and intraretinal electrodes," *Journal of neural engineering,* vol. 11, no. 2, p. 026008, 2014.

[11] Y. H.-L. Luo and L. Da Cruz, "The Argus® II retinal prosthesis system," *Progress in retinal and eye research,* vol. 50, pp. 89-107, 2016.

[12] J. D. Weiland, S. T. Walston, and M. S. Humayun, "Electrical stimulation of the retina to produce artificial vision," *Annual review of vision science,* vol. 2, pp. 273-294, 2016.

[13] A. Hadjinicolaou *et al.*, "Optimizing the electrical stimulation of retinal ganglion cells," *IEEE Transactions on Neural Systems and Rehabilitation Engineering,* vol. 23, no. 2, pp. 169-178, 2014.

[14] Y. S. Goo, J. H. Ye, S. Lee, Y. Nam, S. B. Ryu, and K. H. Kim, "Retinal ganglion cell responses to voltage and current stimulation in wild-type and rd1 mouse retinas," *Journal of neural engineering,* vol. 8, no. 3, p. 035003, 2011.

[15] S. W. Lee, D. K. Eddington, and S. I. Fried, "Responses to pulsatile subretinal electric stimulation: effects of amplitude and duration," *J. Neurophysiol.,* vol. 109, no. 7, pp. 1954-1968, 2013.

[16] Y. J. Yoon *et al.*, "Retinal degeneration reduces consistency of network-mediated responses arising in ganglion cells to electric stimulation," *IEEE Transactions on Neural Systems and Rehabilitation Engineering,* vol. 28, no. 9, pp. 1921-1930, 2020.

[17] A. C. Weitz et al., "Improving the spatial resolution of epiretinal implants by increasing stimulus pulse duration," *Science translational medicine*, vol. 7, no. 318, pp. 318ra203-318ra203, 2015.

[18] W. Li, S. Qin, Y. Lu, H. Wang, Z. Xu, and T. Wu, "A facile and comprehensive algorithm for electrical response identification in mouse retinal ganglion cells," *Plos one*, vol. 16, no. 3, p. e0246547, 2021.

[19] S. Siuly and Y. Li, "Designing a robust feature extraction method based on optimum allocation and principal component analysis for epileptic EEG signal classification," *Comput. Methods Programs Biomed.,* vol. 119, no. 1, pp. 29-42, 2015.

[20] F. A. Elhaj, N. Salim, A. R. Harris, T. T. Swee, and T. Ahmed, "Arrhythmia recognition and classification using combined linear and nonlinear features of ECG signals," *Comput. Methods Programs Biomed.,* vol. 127, pp. 52-63, 2016.

[21] R. G. Afkhami, G. Azarnia, and M. A. Tinati, "Cardiac arrhythmia classification using statistical and mixture modeling features of ECG signals," *Pattern Recog. Lett.,* vol. 70, pp. 45-51, 2016.

[22] L. Li, R. J. Hansman, R. Palacios, and R. Welsch, "Anomaly detection via a Gaussian Mixture Model for flight operation and safety monitoring," *Transportation Research Part C: Emerging Technologies,* vol. 64, pp. 45-57, 2016.

[23] S.-J. Chen, M. Mahadevappa, R. Roizenblatt, J. Weiland, and M. Humayun, "Neural responses elicited by electrical stimulation of the retina," *Transactions of the American Ophthalmological Society,* vol. 104, p. 252, 2006.